Modelling of ductile failure in metal forming

H.H. Wisselink, J. Huetink
Materials Innovation Institute (M2i) / University of Twente,
Enschede, The Netherlands

Summary:

Damage and fracture are important criteria in the design of products and processes. Damage models can be used to predict ductile failure in metal forming processes. Nonlocal models avoid the mesh dependency problems of local damage models. A nonlocal damage model has been implemented in LS-DYNA using the user-subroutines UMAT and UCTRL1. The implemented model will be compared with results obtained with the available option in LS-DYNA to combine *MAT_PLASTICITY_WITH_DAMAGE with *MAT_NONLOCAL. Advantages and disadvantages of the different implementations will be discussed. The user nonlocal damage model has been applied to a bending and a blanking process. Results of these simulations will be shown.

Keywords:

Ductile failure, Nonlocal damage, Bending, Blanking

1 Introduction

Damage and fracture are important criteria in the design of products and processes. Damage models can be used to predict the ductile failure in metal forming processes. However damage softening material models suffer from a pathological mesh dependence upon localisation. The width of the localisation band depends on the mesh size and has no physical meaning. Nonlocal models avoid the mesh dependency problems of local damage models. Here the width of a localisation band is controlled by an extra material parameter, the length scale. This length scale determines the size of the volume where variables are averaged. Two nonlocal damage models are described in Section 2. These models are tested using a tensile test in Section 3. Advantages and disadvantages of the implementations will be discussed. Next the damage model will be applied to some metal forming processes. Results of simulations of a bending and a blanking process will be shown in respectively Sections 4 and 5.

2 Nonlocal damage models

Two nonlocal models will be used in this paper. First the *MAT_NONLOCAL option available in LS-DYNA and secondly an implementation using user-subroutines. Both methods are based on the same article [1] and will be described in Sections 2.1 and 2.2.

2.1 LS-DYNA *MAT_NONLOCAL model

The *MAT_NONLOCAL model [2] can be applied to a subset of the available elastoplastic material models that include a damage based failure criterion. The state variable(s) f which receive a nonlocal treatment can be selected. The nonlocal increase of a state variable $\dot{f}_r$ at x_r, the center of the element e_r is calculated as:

$$\dot{f}_r(x_r) = \frac{1}{W_r}\int_{\Omega_r} \dot{f}^i_{local} w(x_r - y)dy \approx \frac{1}{W_r}\sum_{i=1}^{N_r} \dot{f}_{local} w_{ri} V_i \tag{1}$$

$$W_r = W_r(x_r) = \int w(x_r - y)dy \approx \sum_{i=1}^{N_r} w_{ri} V_i \tag{2}$$

$$w_{ri} = w(x_r - y) = \frac{1}{\left\{1 + \left(\frac{\|x_r - y_i\|}{L}\right)^p\right\}^q} \tag{3}$$

Ω_r is the neighbourhood of radius L of element e_r (Figure 1(a)). e_i are the N_r elements included in Ω_r. $\dot{f}^i_{local}$, V_i and y_i are respectively the local rate of increase of the state variable, the volume and the center of element e_i. The weighting function w_{ri} for different values of parameters p and q is shown in Figure 1(b), however only the default values $p = 8$ and $q = 2$ will be used. The search of the nearest neighbours can take a significant amount of computation time. Therefore this search is normally performed only every n-th increment (typical 10-100).

Here the material model *MAT_PLASTICITY_WITH_DAMAGE (*MAT_81) is used together with the option *MAT_NONLOCAL. The damage ω initiates when the plastic strain reaches $\varepsilon^{failure}$ and grows linearly till complete failure at $\varepsilon^{rupture}$.

$$\omega = \frac{\varepsilon_p - \varepsilon^{failure}}{\varepsilon^{rupture} - \varepsilon^{failure}} \quad \text{if } \varepsilon^{failure} \le \varepsilon_p \le \varepsilon^{rupture} \tag{4}$$

The nonlocal model can be applied on the plastic strain or the damage variable.

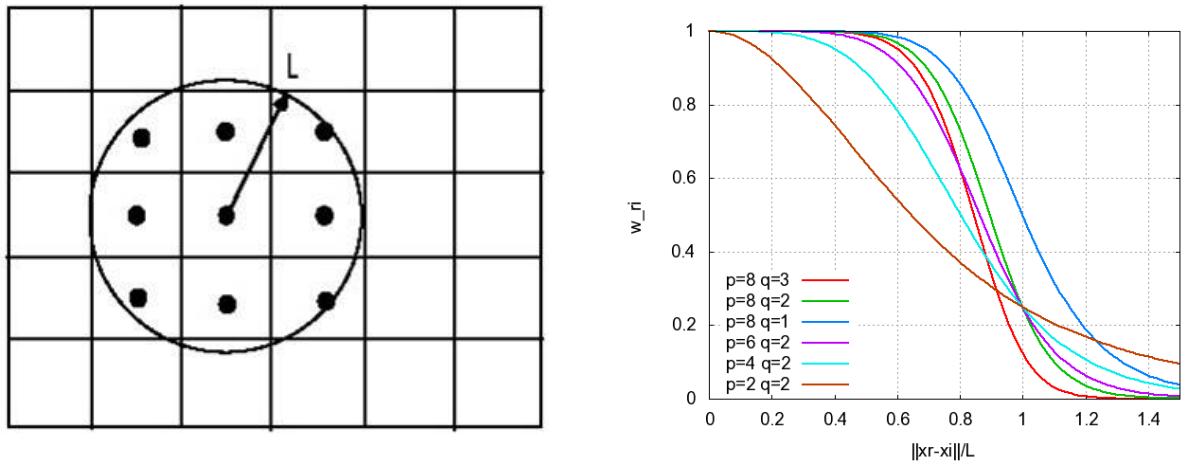

(a) Definition of L

(b) shape of w_{ri}

Figure 1: *MAT_NONLOCAL model.

2.2 USER nonlocal model

The nonlocal damage model presented here is based on the work of Mediavilla [3]. The local damage driving variable z is a function of the local stress and strain history as defined in Equation 5. The triaxiality $\frac{\sigma_h}{\sigma_{eq}}$ in this equation proves to be important factor [4].

$$z = \int_{\varepsilon_p} \langle 1 + A\frac{\sigma_h}{\sigma_{eq}} \rangle \varepsilon_p^B d\varepsilon_p \tag{5}$$

The nonlocal damage driving variable $\bar{z}$ is obtained using a Helmholtz partial differential equation with a Neumann boundary condition (Equation 6). l is the internal length scale, which controls the width of the localisation bands and $\mathbf{n}$ the outward normal on the boundary Γ.

$$\bar{z} - l^2\nabla^2\bar{z} = z; \quad \nabla\bar{z}\cdot\mathbf{n} = 0 \quad \text{on } \Gamma \tag{6}$$

The evolution of history parameter κ is according the Kuhn-Tucker loading-unloading conditions.

$$\dot{\kappa} \geq 0; \quad \bar{z} - \kappa \leq 0; \quad \dot{\kappa}(\bar{z} - \kappa) = 0 \tag{7}$$

The degradation of the material properties ω is calculated from the history parameter κ using a damage evolution law. Here a linear law is used, the degradation initiates at κ_i and the material fails completely at κ_u.

$$\omega = \begin{cases} 0 & \text{for} \quad \kappa < \kappa_i \\ (\kappa - \kappa_i)/(\kappa_u - \kappa_i) & \text{for} \quad \kappa_i \leq \kappa \leq \kappa_u \\ 1 & \text{for} \quad \kappa > \kappa_u \end{cases} \tag{8}$$

The yield stress σ_y is calculated using a strain hardening function h, which competes with the softening due to damage.

$$\sigma_y = (1 - \omega)h(\varepsilon_p) \tag{9}$$

This damage model is implemented in LS-DYNA, using the user subroutines UMAT43 and UCTRL1. An operator split method is applied in which the damage is kept constant during an increment. The calculation of the nonlocal damage from Equation 6, requires an implicit linear Finite Element simulation. The assembly and solution of the system of equations (one d.o.f. per node) takes relatively much time

compared to the time needed for one increment in an explicit FEM code. Therefore the nonlocal damage is only updated every n-th (typical 100) increment.

2.3 Crack propagation

Cracks initiate as the degradation (ω) is equal to one and there is no stiffness left. Crack growth is modelled by element erosion, i.e. failed elements are removed from the problem and the simulation is continued on this updated geometry. Element erosion results in mass loss and a faceted crack surface.

This may have a strong influence on the local stress and strain distributions and may lead to to numerical instabilities. This may result in convergence problems using implicit integration, but is attractive for explicit codes due to its simplicity, compared to alternative computational techniques to describe evolving cracks, such as remeshing.

3 Tensile test

Both nonlocal models described in the previous section are tested with a plane strain simulation of a tensile test on a bar with an imperfection shown in Figure 2. The number of elements used is 120 by 16, which gives a mesh size of 0.125x0.0625mm.

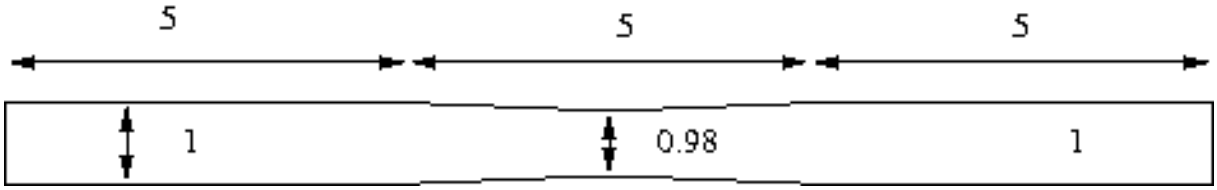

Figure 2: Tensile bar with imperfection, dimensions in mm.

The used hardening function is:

$$h(\varepsilon_p) = 983(\varepsilon_p + 0.041)^{0.256}\,\text{MPa} \tag{10}$$

The influence of the stress state in Equation 5 is neglected by setting $A = B = 0$, which makes z equal to ε_p. Damage ω initiates at $\varepsilon^{failure} = \kappa_i = 0.05$ and grows linearly till complete failure at $\varepsilon^{rupture} = \kappa_u = 0.5$. For local damage both material models yield the same result. Therefore the main difference between the models is the variable which receives the nonlocal treatment.

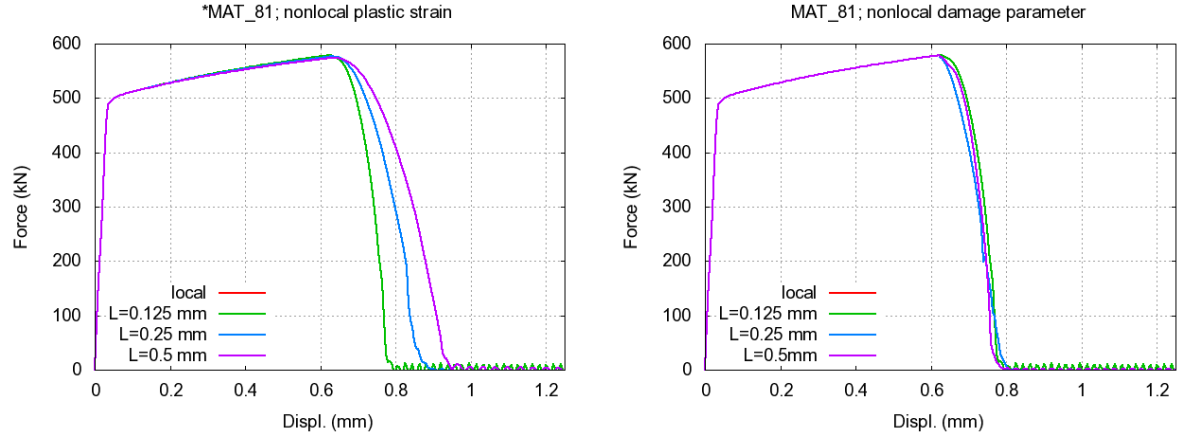

Figure 3: Force-displacement curves for tensile test with *MAT_81 for increasing length scale.

The resulting Force-displacement curves are shown for an increasing length scale for as well a nonlocal plastic strain (Figure 3(left)) as a nonlocal damage (Figure 3(right)). For the smallest length scale $L = 0.125mm$ the results of the nonlocal model converge towards the local model as the number of elements N_r decreases to one. When the length scale increases the case with nonlocal plastic strain shows more ductile behaviour. The width of the localisation bands increases with a lower maximum as can be seen in Figure 4. Note that the mesh even outside the localisation area shows some mesh distortion. Using the nonlocal damage parameter gave a slightly accelerated failure, which was not expected.

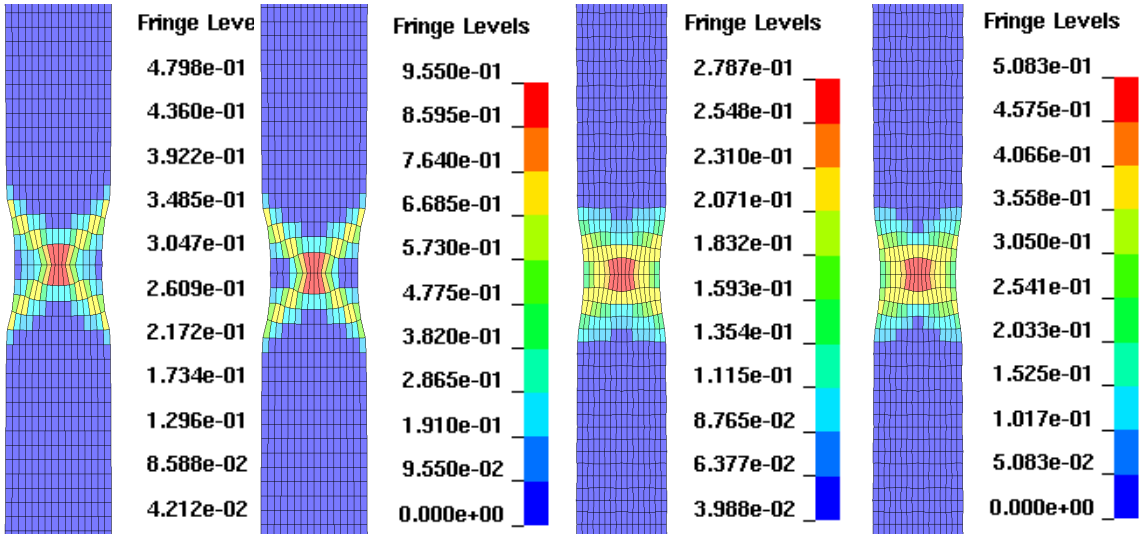

(a) ε_p (b) ω (c) ε_p (d) ω

Figure 4: Results for *MAT_81 with local damage (a,b) and nonlocal plastic strain $L = 0.25mm$ (c,d) at clamp displacement of 0.75 mm, just before fracture.

The calculated force-displacement curves for the user implementation of the nonlocal model (Figure 5) show similar behaviour as the use of a nonlocal plastic strain in *MAT_81. However the final failure is more delayed, which may be attributed to different shapes of the used weighting functions. Also the plastic strain, presented in Figure 6, is not directly changed by the nonlocal treatment, but indirectly through the nonlocal damage driving variable $\bar{z}$ (which is here equal to the nonlocal plastic strain).

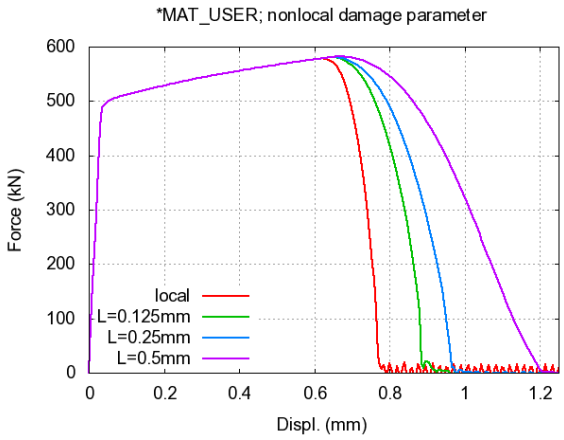

Figure 5: Force-displacement curves for tensile test with *MAT_USER for increasing length scale.

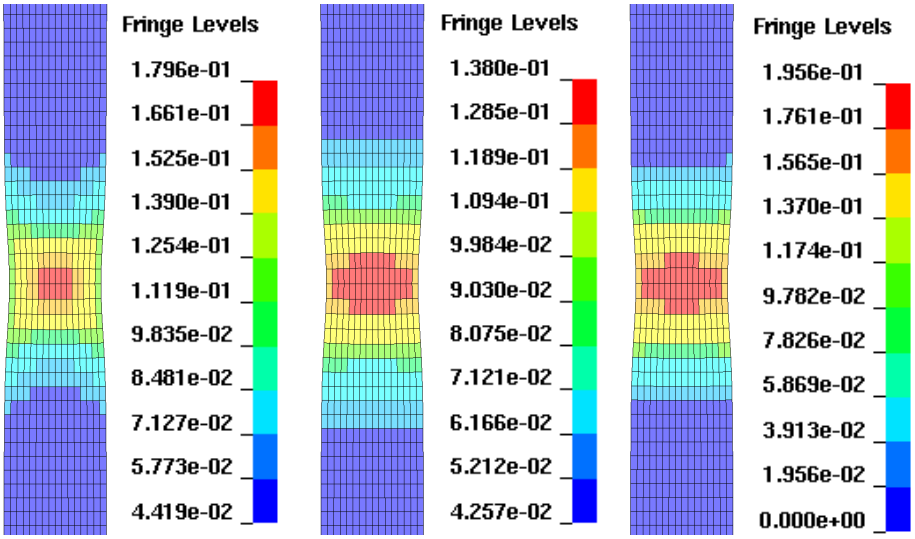

(a) $z = \varepsilon_p$ (b) $\bar{z}$ (c) ω

Figure 6: Results for *MAT_USER at clamp displacement of 0.75 mm; $l = 0.25mm$.

4 Bending

A three-point bending test is used to asses the bendability of a material. A punch with a small radius and a die with a large radius is used (Figure 7(a)). The 1mm thick aluminium sheet is bent until fracture occurs.

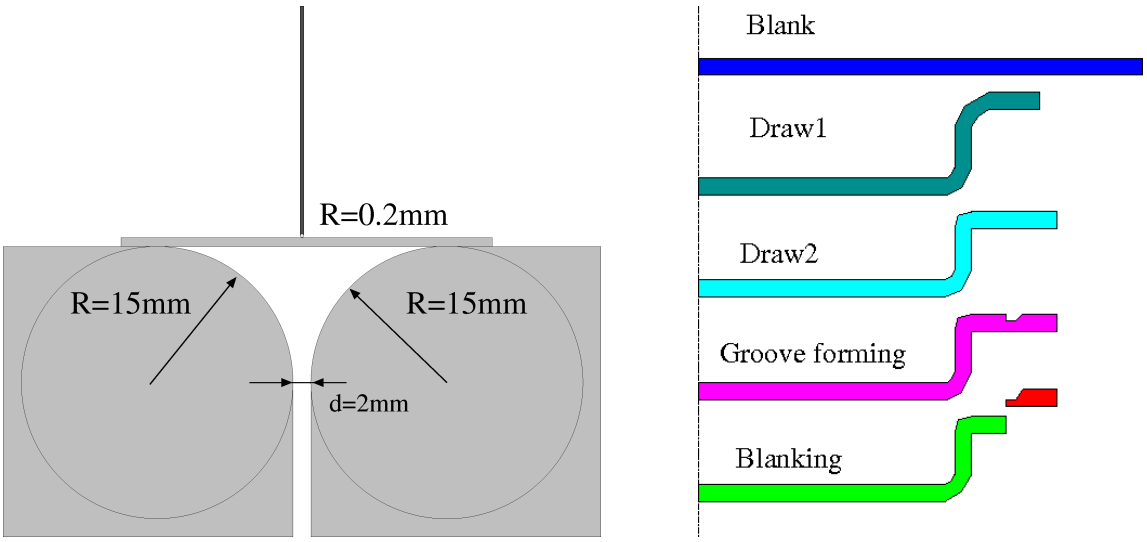

(a) Three point bending (b) Blanking

Figure 7: Schematic view of the modelled forming processes.

A softening mechanism is needed to describe the failure mode - the development of shearbands inclined to the outer surface [5]. Material model *MAT_81 can not be used here as the damage in this model grows as fast in compression as tension, which gives unrealistic results for bending simulations [6]. Therefore the user material model is used here. Taking $A = 3$ and $B = 0$ in Equation 5 gives a faster evolution of the damage under hydrostatic tension than under compression. The hardening curve of the alloy AA6016 is given in Figure 8. The length scale is a material property and should be chosen based on the expected width of a shearband. The element size has to be smaller than the length scale to be effective, which

may lead to very small elements. Therefore in practice some compromise has to be made.

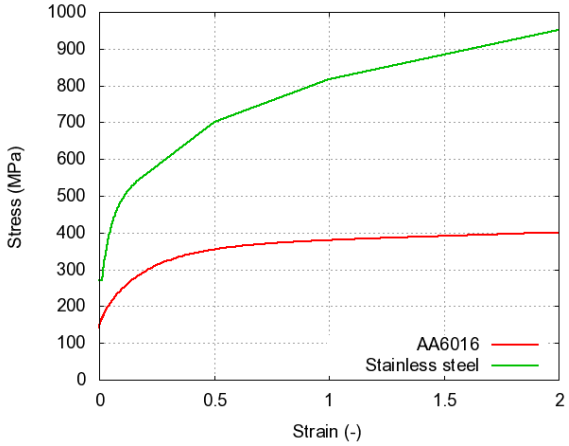

Figure 8: Used stress-strain curves.

The mesh is refined towards the bending zone, which has a uniform mesh with 40 elements in thickness direction of 37.5 by 25 μm. Other simulations showed that a length scale of 50 μm is already too large [7]. Refining the mesh will lead to a drastic increase in calculation time. Therefore here only results are presented using the local damage model. The final failure is shown in Figure 10(a), where two inclined cracks develop at the outer radius In practice only one of these cracks will develop. No damage develops in the inner radius.

In a hemming process the sheet is normally already deformed due to preceding forming operations. This is investigated by applying a 15% uni-axial elongation to the sheet before bending. The pre-straining results in a thickness reduction to 0.938mm and initial values for the plastic strain and damage, ($\varepsilon_p = 0.136$ and $z = 0.273$). Adding a pre-strain to the sheet reduces the bendability as can be seen in Figure 10(b). Here one of the inclined cracks grows further and leads to a complete separation of the parts. The force-displacement curves of bending with and without pre-strain are compared to the experimental ones in Figure 9. One set of parameters gives good results for both cases.

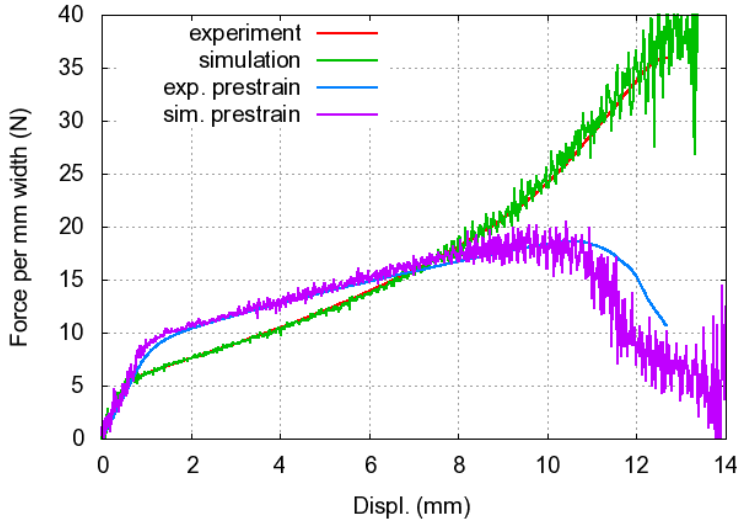

Figure 9: Force-displacement curves of bending with/without prestrain.

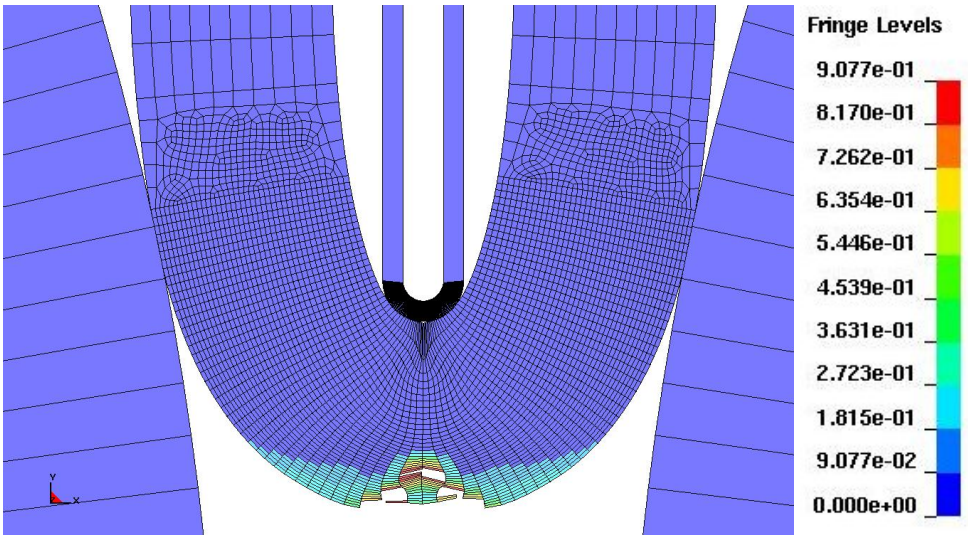

(a) Without prestrain, punch displ. 13.3 mm

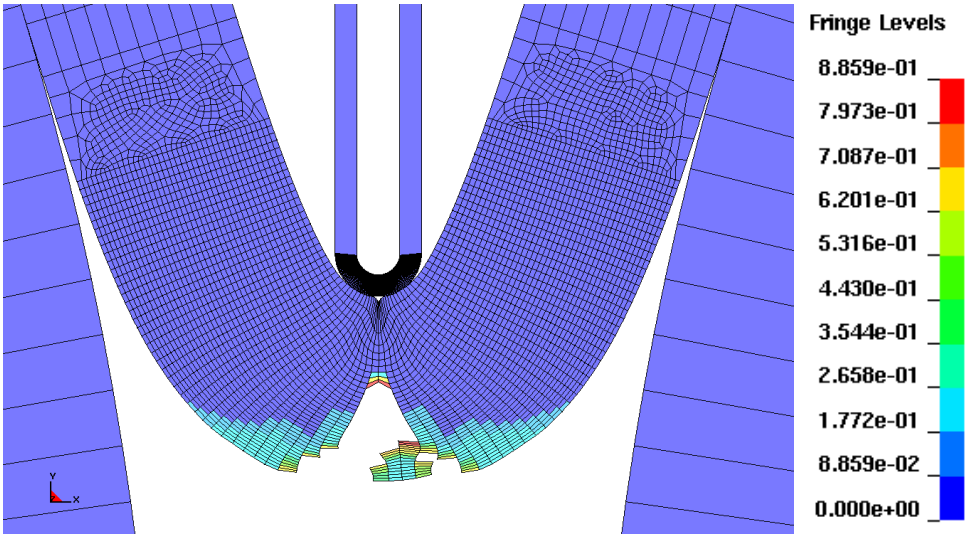

(b) With prestrain, punch displ. 12.9 mm

Figure 10: ω at failure in bending simulation.

5 Burr-free blanking

The last step in a multi step metal forming process using progressive tooling as shown in Figure 7(b) is the separation of the finished parts from the strip of stainless steel (Figure 8). To obtain a burr-free product this blanking process is carried out in two steps. First a groove is pressed into the sheet and next the grooved sheet is blanked from the opposite direction. Now smooth edges are obtained with a fractured part located in the middle of the sheet, where in conventional blanking a burr is formed at one of the edges. This process is modelled to investigate the consequences of the selection of other materials, with different ductility than the currently used ones, on the sheared edge of the product and the robustness of the process.

This blanking process can be approximated with an axi-symmetric model. The drawing steps are modelled separately to obtain an estimate for the state variables before groove forming. Due to the large mesh distortion remeshing is required to perform this simulation (*CONTROL_ADAPTIVE with ADPOPT=-8). At a fixed interval a new mesh is used with equally sized elements of $5\mu m$. In order to keep the number of elements limited the groove forming and blanking are modelled on a ring of material instead of modelling the complete product.

The simulation of the drawing steps gives an estimate of the thickness increase and the reduction of the outer diameter of the flange, which are used to determine the geometry of the ring before groove forming. Furthermore the plastic strain after drawing is taken into account as an initial value (Figure 11(a)). No damage develops in the flange during drawing as the sheet is under compression.

A length scale $l = 10\mu m$ has been chosen, which is twice the element size. Again $A = 3$ and $B = 0$. Several sets of values have been used for the values of κ. Choosing $\kappa_i = 1$ and $\kappa_u = 4$ leads to a premature failure during groove forming as shown in Figure 11. Increasing the values of κ to respectively 2 and 8 increases the ductility. Now the separation of the parts takes place during blanking as intended and a burr-free edge is obtained (Figure 12). This contour agrees with the performed experiments [8].

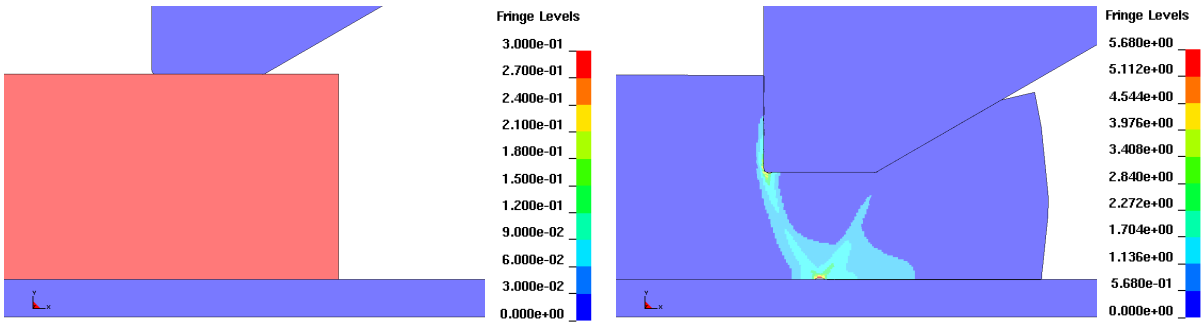

(a) Initial ε_p (b) z before failure

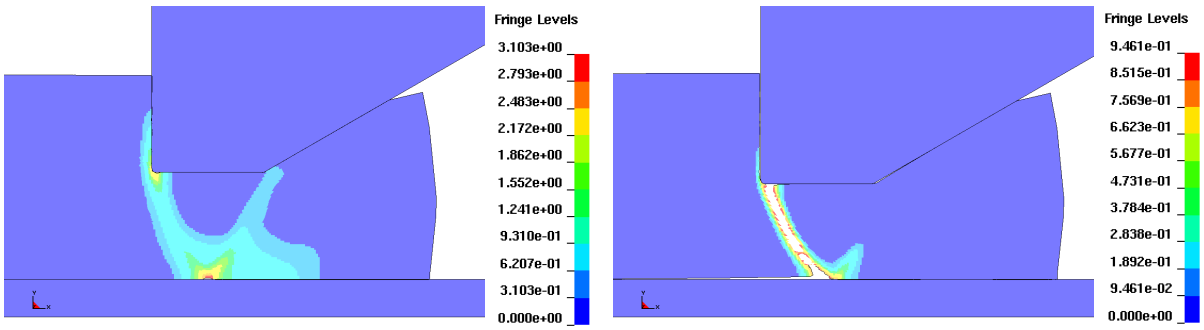

(c) $\bar{z}$ before failure (d) ω after failure

Figure 11: Premature failure in groove forming using $\kappa_i = 1$ and $\kappa_u = 4$.

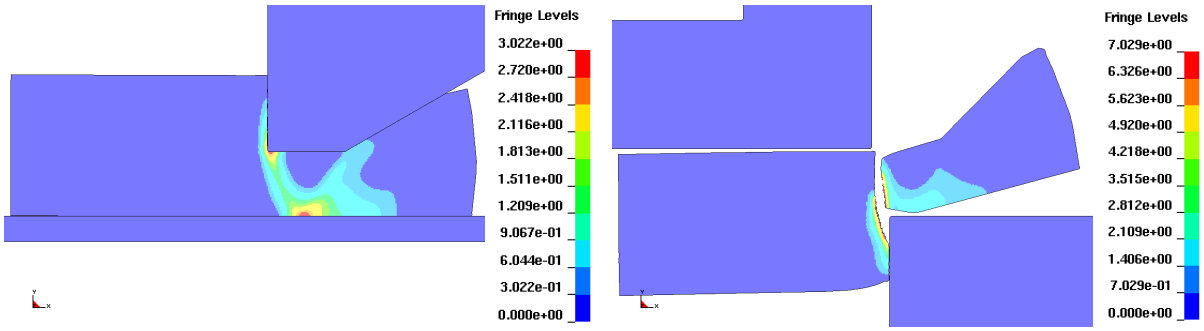

(a) $\bar{z}$ after groove forming (b) ω after blanking

Figure 12: Groove forming and blanking using $\kappa_i = 2$ and $\kappa_u = 8$.

The nonlocal model leads to converging results upon mesh refinement. Remeshing is needed for this simulation, however the remeshing leads to some diffusion of the state variables. Especially around localisation bands this will have an influence on the predicted results.

6 Conclusions

The presented USER nonlocal damage model is able to predict the correct failure modes in the shown examples and gives mesh size independent results. The advantage of the USER model is the more flexible selection of the parameter which gets the nonlocal treatment and it includes the influence of the stress state on the damage evolution.

The USER nonlocal model and the *MAT_NONLOCAL option behave very similar and a combination of *MAT_NONLOCAL with user material models would be interesting.

No standard method exists for the selection of the length scale and the identification of the other parameters of the damage model. Inverse modelling of tests over a range of triaxialities, combined with micro-structural analysis, should give an aswer. However it is difficult to isolate damage effects from strain hardening and other effects.

Modelling localisation bands requires small elements in a small part of the domain for a limited period just before failure. An improved adaptivity may help to reduce the calculation time especially when the nonlocal model is applied to 3D problems.

Acknowledgement

This research was carried out under the project number MC1.05205 in the framework of the Research Program of the Materials innovation institute M2i (www.m2i.nl), the former Netherlands Institute for Metals Research.

7 Literature

[1] G. Pijaudier-Cabot and Z.P. Bazant. Nonlocal damage theory. *J.of Engineering Mechanics-ASCE*, 113(10):1512–1533, 1987.

[2] *LS-DYNA, Keyword User's manual, Version 971*, 2007.

[3] J. Mediavilla, R.H.J. Peerlings, and M.G.D. Geers. An integrated continuous-discontinuous approach towards damage engineering in sheet metal forming processes. *Engineering Fracture Mechanics*, 73(7):895–916, May 2006.

[4] A.M. Goijaerts, L.E. Govaert, and F.P.T. Baaijens. Characterisation of ductile fracture in metal blanking. *J. Mat. Proc. Tech.*, 110:312–323, 2001.

[5] L. Xue and T. Wierzbicki. Ductile fracture initiation and propagation modeling using damage plasticity theory. *Engineering Fracture Mechanics*, 75:3276–3293, 2008.

[6] T. Tsuchida, S. Yamamoto, and K. Isomura. The application of damage & fracture material model to crashworthiness evaluations of aluminum cars. In *4th European LS-DYNA users conference*, 2004.

[7] H.H. Wisselink and J. Huétink. Prediction of the bendability of sheet metals using nonlocal damage models. *Steel research international*, 79(11):217–224, 2008.

[8] H.H. Wisselink, G. Klaseboer, and J. Huétink. Modelling of a burr-free blanking process. In *ESAFORM 2009*, 2009.